

## Steady-State Noises in Diffusion-Limited Fractal Growth.

C. J. G. EVERTSZ(\*) and B. B. MANDELBROT(\*\*)(\*\*\*)

(\*) *Applied Physics Department, Yale University  
Box 2155 Yale Station, New Haven, CT 06520, USA*

(\*\*) *Mathematics Department, Yale University  
Box 2155 Yale Station, New Haven, CT 06520, USA*

(\*\*\*) *Physics Department, IBM T. J. Watson Research Center  
Yorktown Heights, NY 10598, USA*

(received 27 November 1990; accepted in final form 2 April 1991)

PACS. 05.40 – Fluctuation phenomena, random processes, and Brownian motion.

PACS. 64.60A – Renormalization group, fractal and percolation studies of phase transitions.

PACS. 02.50 – Probability theory, stochastic processes, and statistics.

**Abstract.** – The temporal development of patterns in diffusion-limited aggregation (DLA) growth in cylinder geometry is accompanied by various fluctuating quantities. We give experimental evidence that the fluctuations of the highest growth probability and those of the thickness of the interface and of the distance between the highest site and the average height of deposition, have spectra proportional to  $1/f^2$ . There are two or perhaps three crossovers in the exponent, corresponding to the size of the atoms, the thickness of the interface and the width of the cylinder. Fluctuations of very low frequency are not  $1/f^2$ . Thus, the basic Gaussian white noise propelling the Brownian motion of the atoms, interacting with the geometry it creates, is transformed into various  $1/f^2$  noises.

Diffusion-limited aggregation [1] is a special example of a quantized stochastic nonlinear dynamical process, which spontaneously creates fractal [2,3] structures. In this growth process, an atom performs Brownian motion until it hits an initial «seed» (or nucleation point) fixed at the center of the Euclidean plane. At that instant, the seed is modified by embedding this atom, and a fresh Brownian atom is launched against the enlarged target ... and so on. If the aggregate (A) is a perfect conductor kept at a fixed electrostatic potential difference with an electrode (E) at «infinity», the probability of hitting a certain region of the aggregate boundary is well known to be proportional to the electrostatic charge of that region [4-6]. This charge is proportional to the electric field, which is the gradient of the potential [4, 7] obtained by solving the Laplace equation  $\nabla\phi = 0$  in the region between (A) and (E), with boundary conditions, say,  $\phi(A) = 0$  and  $\phi(B) = 1$ . This gradient is called «harmonic measure».

The process is nonlinear and stochastic, because the harmonic measure, a) is determined by the shape of the boundary, and, b) governs in a stochastic manner the discrete change of the boundary in time. The basic quantum of change is the addition of an atom. The source of the stochasticity is Gaussian white noise propelling the Brownian atoms. The influence of noise on the chaotic behavior of deterministic nonlinear dynamical systems, and in particular its role in establishing new types of transitions and/or order, has received much attention (see, e.g., ref. [8, 9]). The key role of noise in establishing the order found in DLA patterns

becomes evident when comparing these patterns with those that arise from a deterministic nonlinear coupling between the harmonic measure and the boundary dynamics (see, *e.g.*, ref. [10] and [11]).

The DLA growth process can start from an arbitrarily shaped seed. In the cylinder geometry [3, 12, 13], growth starts from the bottom side,  $L$  atoms long, of an infinitely elongated rectangle, whose long sides are identified to form a cylinder. A picture of a cluster on a cylinder ( $L = 64$ ) is shown lying on one of its long sides at the bottom of fig. 1. As more Brownian atoms are added, the correlation length increases and by the time the average height is of the order  $L$ , a steady state [12, 13] sets in, and continues indefinitely. In this steady state, many properties of DLA, such as the maximum growth probability, fluctuate around well-defined average values. Therefore, we expect each of these characteristics of DLA to be a *stationary random process*.

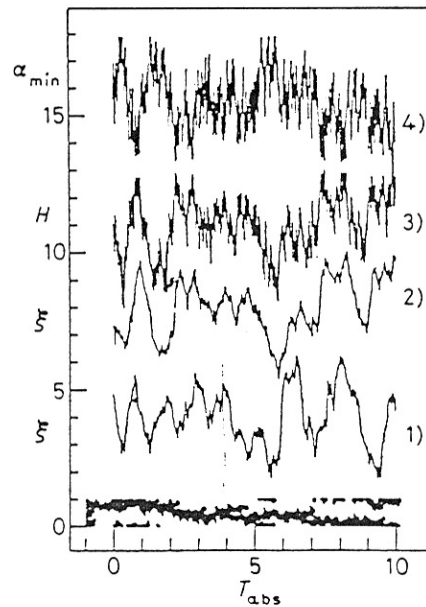


Fig. 1. – A cluster consisting of 8220 atoms of size  $1/64$ . Growth starts at  $T_{\text{abs}} = -1$ , but both growth time and absolute time start at 0, which marks the onset of the steady state. The time series 1) and 2) of the interface thickness  $\xi$  are, respectively, for  $L = 64$  and  $32$ . The series 3) of  $H$  and 4) of  $\alpha_{\min}$  are both for  $L = 32$ . The number of growth time steps for  $L = 64$  and  $L = 32$  are, respectively, 7459 and 2296. The vertical scale is explained in the text.

This letter reports and discusses quantitative numerical evidence, and shows that these processes exhibit long-range time correlations and are characterized by  $1/f^3$  power spectra. Geometric fluctuations with  $1/f^2$  and  $1/f$  were reported in ref. [14] for diffusion fronts, and the occurrence of a  $1/f^2$  power spectrum in circular DLA, associated with «spatio-temporal fluctuations of subclusters» were discussed in ref. [15]. There are very many other examples of phenomena with spectra that follow this law, often with  $\beta \approx 1$  [16-19]. The search for a universal explanation for the recurrence of this spectrum in seemingly unrelated systems has not been successful, and a different explanation may be necessary for each system. We abstain altogether from attempting an analytical explanation of our observations in DLA.

We define *growth time*  $t = 0, 1, 2, \dots$  as the number of atoms in a DLA cluster. At each time  $t$  there is a distribution of growth probabilities  $\{\mu_i\}_{i=1}^{N_t(t)}$  on the cluster's  $N_t(t)$  nearest-neighbor sites. The maximum probability will be denoted by  $\mu_{\max}(t)$ , and its corresponding Hölder by  $\alpha_{\min}(t) = -\ln \mu_{\max}(t) / \ln L$ . The site carrying this maximum is referred to as the cluster's tip, and its height is denoted by  $h_{\max}(t)$ . We define  $h_j$  as the height of the  $j$ -th

nearest-neighbor site,  $N(L)$  as the number of time steps in the series, and average height as  $\langle h \rangle(t) = \sum_{j=1}^{N_f(t)} \mu_j h_j$ . Since we are interested in steady-state properties, we set  $t=0$  when the cluster height reaches  $L$  (see fig. 1). We have studied the following time series:

1) the Hölder series

$$\{\alpha_{\min}(t)\}_{t=1}^{\infty} = \{\alpha_{\min}(0), \alpha_{\min}(1), \alpha_{\min}(2), \dots\};$$

2) the distance  $H(t)$ , at growth time  $t$ , between the average height of deposition of the Brownian atoms and the tip, namely

$$\{H(t)\}_{t=1}^{N(L)} = \{h_{\max}(t) - \langle h \rangle(t)\}_{t=1}^{N(L)};$$

3) the interface thickness, *i.e.*  $\xi(t) = \sqrt{\langle h^2 \rangle(t) - \langle h \rangle^2(t)}$ , which is also equal to the variance of  $H$

$$\{\xi(t)\}_{t=1}^{N(L)} = \{\sqrt{\langle (h_{\max}(t) - h)^2 \rangle - \langle h_{\max}(t) - h \rangle^2}\}_{t=1}^{N(L)}.$$

One glance at fig. 1 suffices to show that the two time series of  $\xi(t)$  are very similar in appearance. The most striking fact is that the relative amount of energy in the high frequencies decreases conspicuously from  $\alpha_{\min}(t)$  to  $H(t)$ , and on to  $\xi(t)$ . The reader familiar with the visual appearance of  $1/f$  noises will be tempted to evaluate the spectra of our records. This will be done momentarily and will indeed prove to yield nearly straight plots. All the time series discussed in this letter have been obtained from square lattice DLA. The harmonic measure was estimated by iteratively solving the discrete Laplace equation [4] to a relative precision 0.0001.

Let us, however, first elaborate on a notion of absolute space and time. The term *absolute time*,  $T_{\text{abs}}$ , will denote the height of the tip  $h_{\max}$ , as measured in units of the cylinder circumference  $L$ . In these units, the atom size is  $1/L$  and the cylinder circumference is 1, so that one unit of absolute time corresponds to the highest cluster site moving over an absolute distance about 1 (see fig. 1). These notions are natural to this process, since its properties only depend on the ratio between the size of the atom and the cylinder circumference. Using  $T_{\text{abs}}$  makes *a priori* knowledge of the rate of addition of atoms unnecessary. When the size of the atoms is decreased (*i.e.* increasing  $L$ ), higher-frequency spectral properties of the various quantities are revealed. Whether, in doing so, the lower-frequency aspects of these quantities remain unchanged depends on the degree of self-similarity of the DLA process.

The time series plotted in fig. 1 have the same duration  $T_{\text{abs}} = 10$ , but different numbers of growth time steps (*i.e.* atoms). The time series (1) for  $L = 64$  contains  $N(L = 64) = 7459$  time steps, while  $N(L = 32) = 2296$  for the series 2), 3) and 4). Doubling  $L$  going from series 1) to 2) increases the time resolution by a factor  $2^D$ , where  $D \approx \ln_2 \{N(L = 64)/N(L = 32)\} \approx 1.7$ . In drawing fig. 1 we subtract the averages  $\langle \xi(L = 64) \rangle = 10.11$ ,  $\langle \xi(L = 32) \rangle = 5.09$ ,  $\langle H(L = 32) \rangle = 4.89$  and  $\langle \alpha_{\min}(L = 32) \rangle = 0.73$  from the respective time series 1) to 4), and divided by their respective variances 1.31, 1.00, 0.99 and 0.04. To avoid overlap we added 4 to the series  $\xi(L = 64)$ , 8 to  $\xi(L = 32)$ , 18 to  $H(L = 32)$  and 12 to  $\alpha_{\min}(L = 32)$ .

In the steady state, the height of the cluster, and thus absolute time, is in the *average* proportional to growth time  $t$ , namely

$$T_{\text{abs}} \sim tL^{-D}. \quad (1)$$

In practice, we perform the spectra analysis on growth time series for which the addition of one atom determines a *time step*. This introduces a lower cut-off to the absolute time, and thus an upper cut-off to relevant frequencies. Therefore, it is important to know the relation between  $t$  and the absolute time in more detail. Note that this relation is independent of the rate of addition of the atoms, and also applies to physical experiments as long as atoms are added one at the time.

The probability density  $\Gamma_L(t)$  of tip life times, which is proportional to the number of instances in which the site with the largest growth probability survived  $t$  time steps in the steady state, was studied for  $L = 32, 64$  and  $L = 128$ . Each data set was gathered for a duration  $T_{\text{abs}} = 10$ . The number of time steps involved were, respectively,  $N(L = 32)$ ,  $N(L = 64)$  and  $N(L = 128) = 24407$ . The approximate straightness we observed in plots of  $\ln \Gamma_L(t)$  vs.  $t$  suggests that the distribution  $\Gamma_L(t)$  follows an exponential of the form  $\Gamma_L(t) = \zeta \exp[\zeta] \exp[-\zeta t]$ . The tips have therefore a characteristic growth lifetime  $\tau = 1/\zeta$  with a finite variance  $1/\zeta^2$ , and thus move with a well-defined average velocity. For our three cylinder circumferences we have estimated  $\zeta(32) \approx 0.1415$ ,  $\zeta(64) \approx 0.0892$  and  $\zeta(128) \approx 0.0534$ . These values are in reasonable agreement with the expected behaviour  $\tau(L) = 1/\zeta(L) = AL^{D-1}$ , where  $A$  is a prefactor. We therefore expect the texture of absolute time, followed in growth time, to be smooth above the absolute time scale  $\tau(L)/L^D \sim L^{-1}$ , while the roughening below this length scale causes crossovers in the spectral densities at frequency  $\Omega_3(L) \sim L$ .

Now we move on to the spectral densities  $P_x(f)$  of the growth time series. These were estimated by fast Fourier transform [20] on the doubled and mirrored form of the series  $\{\{x(t)\}_{t=1}^{N(L)}, \{x(t)\}_{t=N(L)}^1\}$ , with  $x = \xi, H$  or  $\alpha_{\min}$ . The plots of  $\ln P_x(f)$  vs.  $\ln f$  for  $x = \xi, H, \alpha_{\min}$  and  $L = 32, 64, 128$  are shown in fig. 2. The circles mark the  $L = 128$  results. The resemblance between the behavior of the spectra for different  $L$  suggests that the behavior of the fluctuations above the atomic scale does not depend on that scale. The collective behavior of a large number of small atoms somehow becomes integrated to yield the behavior of larger atoms [21, 22].

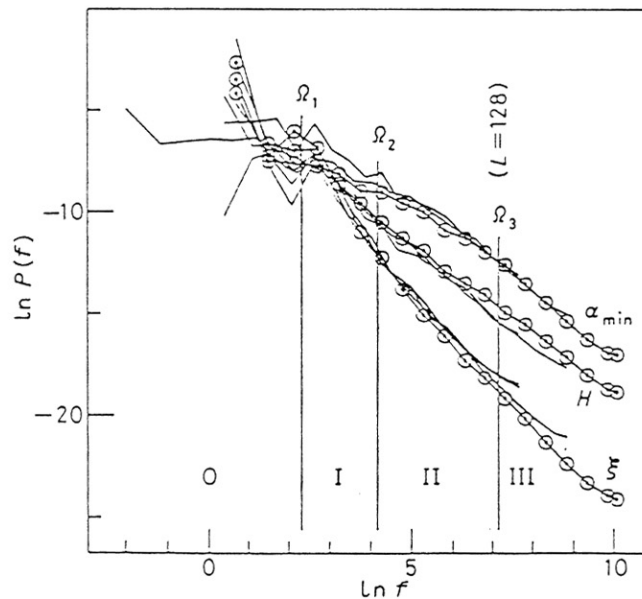


Fig. 2. – The spectral densities for  $\xi, H$  and  $\alpha$  for cylinder circumferences  $L = 32, 64, 128$ . The 128 data is marked by circles. From left to right the vertical lines mark the crossover frequencies for  $L = 128$ . They correspond to the cylinder width, the interface thickness and the size of an atom. The resulting frequency windows O, I, II and III are discussed in the text.



One can distinguish three frequency ranges, each yielding a different form of the spectrum. The fluctuations in the time series considered are caused by the change in the geometry due to the addition of atoms. In a geometrical sense the change is always the same, namely, the addition of one atom. However, quantities like  $\xi$ ,  $H$  and  $\alpha_{\min}$  involve the harmonic measure, hence one can expect larger changes when the arriving atom reshapes the region near the tip than far away from it. To see that this may introduce another crossover, let  $\langle H(L) \rangle$  be the time-averaged height difference between the tip and the average point of attachment of the Brownian atom. Now, although the interaction of the potential field with the geometry is of infinite range, it can only manifest itself in the fluctuations of the quantities, through the arrival of atoms. The fact that this arrival is limited by Faraday screening causes the emergence of the length scale  $\langle H(L) \rangle$ . This corresponds with an absolute time scale  $\langle H(L) \rangle / L \sim 1/\Omega_2$ . Now, the quantity  $\langle H(L) \rangle$  is expected to be of the same order of magnitude as  $\langle \xi(L) \rangle$ . Indeed, we find numerically that in growth units,  $\langle H(L=32, 64, 128) \rangle = 4.89, 9.40, 18.12$  and  $\langle \xi(L=32, 64, 128) \rangle = 5.1, 10.1, 20.0$ . This data also confirms that both quantities scale with  $L$  [3, 12], so that  $\Omega_2$  is a constant frequency. One therefore expects that fluctuations in this «Faraday» range (II), between  $\Omega_2$  and  $\Omega_3(L)$ , are correlated by the long-range Laplacian interaction. These correlations are also present above  $\Omega_3(L)$ , but are masked by the roughness of the absolute time. Frequencies above  $\Omega_3(L)$  correspond to fluctuations that occur when the atoms attach below the tip while the latter does not move. We call the frequencies  $\geq \Omega_3(L)$  the subatomic range (III).

There are however also correlations arising from the memory carried by cluster morphology. The concept of *geometric memory* is elucidated by the exemplary thought experiment in which DLA growth starts from a line segment in the center of the circular geometry. After the addition of enough atoms, the active zone where the majority of the atoms attach does not anymore include this initial line. Nevertheless, the elliptic-shaped envelope of this active zone still carries the geometric memory of the initial seed. This we believe accounts for the correlations on length scales way above  $\langle H(L) \rangle$ , which are clearly visible in fig. 1.

From the 4 leftmost data points in the subatomic range (III) of the  $L=128$  data, we estimated  $P(f) \sim f^{-\beta}$ , with

$$\beta_{\text{III}}(\alpha_{\min}) \approx 1.8, \quad \beta_{\text{III}}(H) \approx 1.5, \quad \beta_{\text{III}}(\xi) \approx 2.1. \quad (2)$$

In the Faraday range (II) where both sources of correlation are expected to be present, we find numerically the following for  $L=32, 64, 128$ :

$$\beta_{\text{II}}(\alpha_{\min}) \approx 1.1 \pm 0.1, \quad \beta_{\text{II}}(H) \approx 1.5 \pm 0.1, \quad \beta_{\text{II}}(\xi) \approx 2.3 \pm 0.1. \quad (3)$$

Except for  $\alpha_{\min}$ , there is no marked difference between the exponents  $\beta$  in the ranges II and III. However, if one superposes the tails of the spectra in range III, one finds that they behave very similarly for all three values of  $L$ . This suggests that, contrary to the range II, the values of  $\beta$  in range III may be the same.

It seems clear that for finite  $L$ , there should be a finite lower cut-off frequency  $\Omega_1(L)$  to the range (I) between  $\Omega_1(L)$  and  $\Omega_2(L)$ . In this range the only source of correlation is the geometric memory. To estimate the value of  $\Omega_1(L)$ , we made a long ( $T_{\text{abs}} = 120$ ) time series  $\xi'$  for  $L=32$ . This is expected to suffice, since, as remarked earlier, the low-frequency behavior of the spectra appear to be independent of  $L$ . We found the high-frequency parts of  $\xi'$  to be very much the same as those for the series  $\xi(L=32)$ . The  $T_{\text{abs}} = 10$  series are thus clearly long enough to provide enough statistics for frequency ranges II and III. The low-frequency part of the spectrum of  $\xi'$ , which is the curve reaching far most to the left in fig. 2,

suggests that the spectrum is flat for length scales above  $L$ . The same behavior was also found for the long series of  $H$  and  $\alpha_{\min}$ . We therefore took  $\Omega_1 \approx L$  in fig. 2. For the range I, we remark that for  $\alpha_{\min}$  the exponent  $\beta$  seems to decrease when going from range II to I, while for  $\xi$  the opposite happens.

Correlations between the series in fig. 1 become clearly visible when comparing the series 2), 3) and 4) in fig. 1. When  $\alpha_{\min}$  is small, i.e.  $\mu_{\max}$  is large, the tip lies highest above the average height  $\langle h \rangle$ , and causes an increase in the standard deviation  $\xi$  of  $h$ . Small  $\alpha_{\min}$  are therefore expected to be accompanied by large  $\xi$  (anti-correlation), while  $\xi$  and  $H$  are expected to be correlated. From the difference in the behavior of their respective spectral densities, one can infer that these correlations are caused by a *nonlinear* dependence between the quantities, the exact nature of which is presently unclear.

This letter has discussed numerical evidence for the existence of  $1/f^3$  noises in steady-state DLA. There seem to be four length scale domains, with different spectral density exponents: 0) above the cylinder circumference  $L$ , I) between  $L$  and the interface thickness  $\xi$ , II) between  $\xi$  and the atomic size and III) below the atomic size. These noises are spontaneously generated in the DLA fractal growth process which is driven by Gaussian white noise.

\* \* \*

We would like to thank Dr. J. W. COOLEY for allowing us to use his FFT programs. This research has been financially supported in part by the Office of Naval Research, grant N00014-88-K-0217, and in part by the Geometry Supercomputer Project.

## REFERENCES

- [1] WITTEN T. A. and SANDER L. M., *Phys. Rev. Lett.*, **47** (1981) 1400.
- [2] MANDELBROT B. B., *Fractal Geometry of Nature* (Freeman and Company, San Francisco, CA) 1982.
- [3] MEAKIN P., in *Phase Transitions and Critical Phenomena*, Vol. 12, edited by C. DOMB and J. LEBOWITZ (Academic Press, New York, N.Y.) 1988, p. 335.
- [4] NIEMEYER L., PIETRONERO L. and WIESMANN H. J., *Phys. Rev. Lett.*, **52** (1984) 1033.
- [5] KAKUTANI S., *Proc. Imp. Acad. Sci. (Tokyo)*, **20** (1944) 706.
- [6] PIETRONERO L. and WIESMANN H. J., *J. Stat. Phys.*, **36** (1984) 909.
- [7] MANDELBROT B. B. and EVERTSZ C. J. G., *Nature (London)*, **348** (1990) 143.
- [8] HORSTHEMKE W. and LEFEVER R., *Noise-Induced Transitions* (Springer-Verlag, Berlin) 1984.
- [9] MOSS F. and MCCLINTOCK P. V. E. (Editors), *Noise in Nonlinear Dynamical Systems*, Vol. 1-3 (Cambridge University Press, Cambridge) 1989.
- [10] BENSIMON D., KADANOFF L. P., LIANG S., SHRAIMAN B. I. and TANG C., *Rev. Mod. Phys.*, **58** (1986) 977.
- [11] SANDER L. M., RAMANLAL P. and BEN-JACOB E., *Phys. Rev. A*, **32** (1985) 3160.
- [12] EVERTSZ C. J. G., *Phys. Rev. A*, **41** (1990) 1830.
- [13] EVERTSZ C. J. G., *J. Phys. A*, **22** (1989) L-1061.
- [14] GOUYET J. F., SAPOVAL B., BOUGHALEB Y. and ROSSO M., *Physica A*, **157** (1989) 620.
- [15] ALSTRØM P., TRUMFIO P. A. and STANLEY H. E., *Phys. Rev. A*, **41** (1990) Rap. Com. 3403-3406.
- [16] VOSS R. F., *Fundamental Algorithms for Computer Graphics*, NATO ASI Series, Vol. F17, edited by R. A. EARNSHAW (Springer, Berlin) 1985.
- [17] BAK P., TANG C. and WIESENFIELD K., *Phys. Rev. Lett.*, **59** (1987) 381.
- [18] WEISSMAN M. B., *Rev. Mod. Phys.*, **60** (1988) 2, 537.
- [19] HWA T. and KARDAR M., *Phys. Rev. Lett.*, **62** (1989) 1813.
- [20] SINGLETON R. C., *IEEE Trans. Audio Electroacoustics*, **17** (1969) 2, 93.
- [21] PIETRONERO L., ERZAN A. and EVERTSZ C. J. G., *Phys. Rev. Lett.*, **61** (1988) 861; *Physica A*, **151** (1988) 207; EVERTSZ C. J. G., *Laplace Fractals*, Groningen Ph.D. thesis (1989).
- [22] BARKER P. W. and BALL R. C., *Real Space Renormalization of DLA*, preprint (1990).